Available online at www.sciencedirect.com
ScienceDirect
Journal of the European Ceramic Society 31 (2011) 1067–1074
www.elsevier.com/locate/jeurceramsoc

Original Article

Inkjet printing of photocatalytically active TiO_2 thin films from water based precursor solutions

Melis Arin [a], Petra Lommens [a], Nursen Avci [b], Simon C. Hopkins [c], Klaartje De Buysser [a], Ioannis M. Arabatzis [d], Ioanna Fasaki [d], Dirk Poelman [b], Isabel Van Driessche [a,*]

[a] *SCRIPTS, Department of Inorganic and Physical Chemistry, Ghent University, Krijgslaan 281 (S3), 9000 Ghent, Belgium*
[b] *LUMILAB, Department of Solid State Sciences, Ghent University, Krijgslaan 281 (S1), 9000 Ghent, Belgium*
[c] *Department of Materials Science and Metallurg, University of Cambridge, Pembroke Street, Cambridge CB2 3QZ, United Kingdom*
[d] *NanoPhos SA, PO Box 519, Science & Technology Park of Lavriou, Lavrio 19500, Attica, Greece*

Received 27 August 2010; received in revised form 10 December 2010; accepted 21 December 2010
Available online 28 January 2011

Abstract

In this work, aqueous chemical solution deposition route suited for inkjet printing is used for the synthesis of photocatalytically active TiO_2 coatings. Environmentally friendly precursor solutions with electromagnetic ink-jet printing, allows cheap and simple processing of TiO_2 films on glass. The hydrolysis reaction of water sensitive titanium alkoxide (Ti-alkoxide) precursor is controlled by adding complexing agents as citric acid and triethanolamine prior to water addition, and aqueous stable solutions are achieved. The pH of the solutions is brought to neutral to guarantee flexible processing, avoid damage to substrates and equipment. Solution parameters are adapted to obtain optimal gelation conditions and good jettability. The influence of processing parameters on the phase formation and surface morphology is studied by thermogravimetric analysis and differential thermal analysis (TGA/DTA), X-ray diffraction (XRD), scanning electron microscopy (SEM) and atomic force microscopy (AFM). The photocatalytic activity of the films is evaluated by the degradation of methyl orange.

Keywords: Films; Chemical properties; Sol–gel processes; TiO_2; Inkjet printing

1. Introduction

In recent years, titanium dioxide, a high energy band gap semiconductor, has received considerable interest due to its photocatalytic activity under UV-irradiation. As TiO_2 layers are transparent and colorless, more and more applications become available for TiO_2. Thin TiO_2 coatings can be used to create self-cleaning, antifogging, and superhydrophilic surfaces.[1–7] Combined with its high refractive index, it is one of the most promising wide band gap semiconductors for use in optoelectronics such as solar cells.[1,8–10]

TiO_2 films prepared by chemical solution deposition methods are attracting much attention, because of the relatively simple production of large area, high purity films at low cost and high scalibility.[11–14] At this time, most of the sol–gel chemistry literature on TiO_2 focuses on controlled hydrolysis in alcoholic media.[15–19] However, industrial demands encourage the development of water based precursor designs. The difficulty lies in the high reactivity of Ti-alkoxide towards H_2O. In organic media, hydrolysis is often induced by adding small amounts of H_2O. Yet, we want to avoid this hydrolysis and the resultant precipitation by blocking the hydrolysis reaction in pure aqueous media, using complexing ligands as stabilizing agents. We choose triethanolamine (TEA) and citric acid (CA) which are used in cosmetics and food industry respectively and thus are environment-friendly. So far there are a limited number of publications on aqueous TiO_2 solutions starting from alkoxides such as the study of Ohya et al. where different complexing agents like amines and carboxylic acids were used to create precursor solutions suited for spincoating on glass.[4] In Sheng's study,[20] H_2O was used in high molar ratios for the hydrolysis of Ti alkoxide, however peptization was done with HNO_3 at very low pH values (1–2). This is in line with a number of studies,[15–20] where the pH levels of the solutions necessary to stabilize Ti^{4+} ion, are below

* Corresponding author. Tel.: +32 9 264 44 33; fax: +32 9 264 49 83.
E-mail address: Isabel.VanDriessche@UGent.be (I. Van Driessche).

0955-2219/$ – see front matter © 2011 Elsevier Ltd. All rights reserved.
doi:10.1016/j.jeurceramsoc.2010.12.033

5. These low pH values are unfavorable, since they complicate further industrial handling, can damage the substrate, and might influence phase formation. In Truijen's studies,[6,7] Ti^{4+} ions can only be stabilized at neutral pH levels in a water based solution using a citratoperoxo method. This method however uses both the citric acid and the highly corrosive H_2O_2 for stabilization. In this study, we focus on fast, economically synthesized, and completely environmentally friendly solutions by eliminating toxic organics as much as possible.

To apply these precursor solutions to the substrate, we have shifted from the commonly used dip coating and spin coating techniques to a completely new approach, ink-jet printing. This is a non-contact deposition method which can be used to obtain large area coverage with direct patterning on almost any substrate. Droplets of the precursor solution are generated and placed on the substrate according to the selected pattern.[21,22] In this way, both patterned deposits and completely covered surfaces can be generated with the same equipment and precursors. This results in simplicity, low cost, less material waste, and convenient control of the coating. This ink-jet printing based method is in line to industrial needs for robust, high volume and precise deposition of inks.[22]

This study focuses on preparing highly water based stable Ti precursors at neutral pH and with simple complexing agents, inkjet printing the solutions on glass substrates, and sintering at low temperature (500–650 °C), to transform the wet printed layers to the final transparent, thin, and dense TiO_2 layers.

2. Experimental

2.1. Materials

Aqueous TiO_2 precursor solutions were prepared using tetrabutyl orthotitanate as the Ti source and citric acid, acetylacetone, and triethanolamine as complexing agents. Small amounts of ethanol (EtOH) (Absolute, Panreac) were used to dissolve the metal alkoxide and help to control hydrolysis during water addition. Tetrabutyl orthotitanate (TNBT) (purity ≥97.0%) was purchased from Fluka, citric acid (CA) (purity 99.5%) and triethanolamine (TEA) (purity 99+%) were purchased from Acros Organics. All materials were used without further purification.

2.2. Preparation

Two different precursor solutions were prepared in 50 ml quantities, with CA and TEA as complexing agents, and water as the primary solvent. *Ti-CA solution* – TNBT was dissolved in EtOH in 7:1 molar ratio to Ti^{4+}, and CA was added (2:1 molar ratio to Ti^{4+}) under stirring, at 60 °C. After complete dissolution of CA, the solution was cooled to room temperature and H_2O in 82:1 molar ratio to Ti^{4+}, mixed with EtOH (0.5:1 molar ratio to Ti^{4+}), was added dropwise to the solution in order obtain a final Ti^{4+} concentration of 0.4 M. *Ti-TEA solution* – TEA was added to TNBT (Ti^{4+}:TEA molar ratio of 1:2), under continuous stirring and H_2O in 71:1 molar ratio to Ti^{4+} mixed with EtOH (2:1 molar ratio to Ti^{4+}) was added to the solution. The solution was stirred at 40 °C for 30 min, with a final Ti^{4+} concentration of 0.5 M. Throughout this paper, the solutions are named according to the complexing agents, as solution Ti-CA and solution Ti-TEA.

For solution CA, pH adjustment ($5 < pH < 8$) was done by adding NH_4OH (NH_3 in 25 wt% water). The pH of solution TEA was 9.4 and the precursor was used as such for the reported experiments.

2.3. Printing

For inkjet printing of the precursor solutions, a single Domino Macrojet electromagnetic nozzle with 90 μm diameter jewel orifice, modified in University of Cambridge and mounted on a Roland *x–y* plotter was used. This kind of nozzle can dispense highly viscous (up to 1000 cP), non-magnetic inks, producing >1 nL droplets up to 1 kHz. The pressure was set between 0.3 and 0.8 bar and the deposition was performed at room temperature. The glass substrates used for coating were standard microscope slides with dimensions 20 mm × 50 mm. In this work, we aim at covering 2 cm × 2 cm area with a homogeneous TiO_2 coating. To cover the substrate as efficiently as possible, the single droplets ejected from the nozzle are printed according to a hexagonal droplet array. By optimizing the interdroplet distance in this array (=smallest distance between two neighboring droplets), we can find the optimum balance between merging of droplets to ensure coverage and overlapping of droplets causing undesired inhomogenities in the layer. In this work, the interdroplet distance was varied between 2 and 5 mm to obtain optimum substrate coverage, and the droplets had diameters of ≥1 mm after spreading on the substrate.

After printing the layers were gelated at 60 °C for 3–4 h under air. Sintering was performed in a tube furnace at 500, 550, 600, and 650 °C for 1 h with a heating rate of 5 °C/min under O_2.

2.4. Characterization

The viscosity of the solutions was determined using a Brookfield DVE viscometer. The wettability was studied by measuring the contact angle of a 10 μl droplet of precursor solution on glass substrates, and the surface tension by the pendant drop method using an optical tensiometer (KSV CAM 200). TGA/DTA (TA Instruments SDT) analysis was performed on dried gels with a heating rate of 10 °C/min until 1100 °C under O_2 flow. XRD analysis was performed powders using solid state detector, 0.02° step size, and 1 s step time (Thermo Scientific, detector Arl X'TRA), and on layers on layers using Lynxeye line detector, 0.04° step size, and 2 s step time (Bruker D8, Cu Kα radiation) to check the crystal structure. The homogeneity and smoothness of the films were investigated by SEM (FEI Quanta 200F) and AFM (Molecular Imaging, PicoPlus). The thickness of the films was measured by a spectroscopic ellipsometer (SE, J.A. Woollam Co. Inc., M-2000FI) where the Cauchy dispersion model was used to fit the optical constants. The transparency of the films on glass substrates was determined by UV–vis spectrophotometry (Varian Cary 500). The photocatalytic activity of the sol–gel films was evaluated by following the degradation of methyl orange under UV illumination. The experiments

were carried out in round-bottom photocatalytic cells with a near UV-transparent window (cut off below 340 nm). A laboratory constructed irradiation box equipped with four Sylvania GTE 15W F15W/T8 blacklight blue fluorescent light tubes was used. The photon source has a maximum emission at 360 nm and emits 71.7 $\mu W\,cm^{-1}$ at a distance of 25 cm. The aqueous methyl orange solutions were prepared from Sigma–Aldrich powder (without further purification) and their absorption was set to be at 0.810. The azo-dye solutions were used without prior oxygen gas bubbling. The concentration was correlated to the absorption of the methyl orange solution at 466.5 nm ($\varepsilon_\lambda = 466.5 = 25{,}100\,cm^{-1}\,M^{-1}$), using a single beam Shimadzu UV 1240 spectrophotometer. The titania modified microscopy slides were accurately shaped at 0.8 cm^2 or 2.0 cm^2 and inserted in the photocatalytic cell. Photocatalysis experiment took place under stirring as 25 cm of the light source.

3. Results and discussion

3.1. Aqueous TiO_2 precursor solutions

We have prepared two different aqueous TiO_2 precursor solutions using citric acid (CA) and triethanolamine (TEA) as complexing agents, to inhibit hydrolysis of the Ti-alkoxide. When stored in sealed beakers at room temperature, the Ti-CA and Ti-TEA solutions were stable for several months. This stability is of major importance to the suitability for ink-jet printing: formation of even very small precipitates can block the nozzles. Heating of small amount of the solutions poured into a petri dish to 60 °C for 2 h has lead to stable and transparent gels (see Supporting Information (Fig. S1)). Prior to gelation, the pH of the Ti-CA precursor was adapted to 5, for the Ti-TEA precursor, the best gels could be obtained when working at a pH value around 9.

3.2. Ink-jet printing

The ink-jet printing parameters were chosen according to the rheological properties of the solutions (Table 1). For each solution, the opening time determined the size of each droplet printed on the substrate and was kept constant at an optimized value. Both solutions could be printed successfully on glass substrates without the addition of any wetting agent. Good spreading on the substrate and adherence of the droplets on the glass surfaces was achieved. A lower ink supply pressure needed to be used in order to print good layers for solution Ti-TEA in comparison with solution Ti-CA, as the viscosity of solution Ti-TEA is higher than that of solution Ti-CA, as shown in Table 1. From contact angle measurement we found that droplets of solution Ti-CA and Ti-TEA spread completely on the glass substrates.

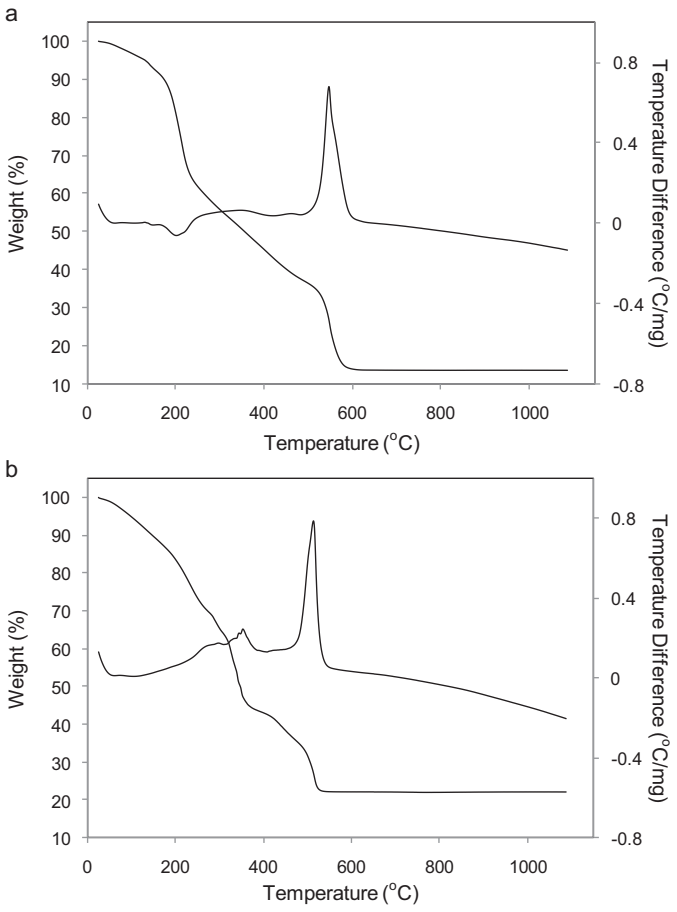

Fig. 1. TGA–DTA spectra obtained for (a) gel Ti-CA and (b) gel Ti-TEA.

Surface tension values (γ) for both solutions were determined by the pendant drop method. Compared to the surface tension of water, which is 72 mN/m, our solutions have a lower surface tension (Table 1) which explains why the droplets spread easily to form a complete layer on the substrate.

3.3. Thermal treatment

Thermal analysis of the precursor gels was performed in order to deduce the heat treatment parameters for the formation of TiO_2 crystallites in the two different gels. For both gels, a continuous mass loss in several overlapping steps was found until a temperature of ~520 °C. The mass losses before 200 °C are related to the evaporation of water, ethanol, and ammonia. For gel Ti-CA (Fig. 1a), an exothermic peak at 540 °C is associated with the decomposition of the citric acid complex.[23] For both graphs, the peak between 270 °C and 350 °C can be attributed to decomposition of butoxide chains.[24] For gel Ti-TEA (Fig. 1b) the exothermic peak around 500 °C relates to the decomposition

Table 1
Ink-jet printing (IJP) parameters with rheological properties of the TiO_2 solutions.

Solution	Viscosity [cP]	Contact angle [°]	Surface tension [mN/m]	IJP pressure [bar]	IJP opening time [μs]	Distance between droplets [mm]
Ti-CA	4.3	≤5	24.6	0.4	100	5
Ti-TEA	5.2	≤5	25.3	0.3	50	2

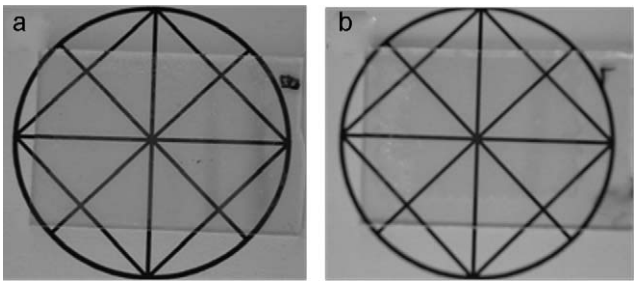

Fig. 2. TiO_2 layers on glass obtained by printing and subsequent sintering at 500 °C of (a) solution Ti-CA and (b) solution Ti-TEA.

of the Ti-TEA complex. The lower peak intensities for Ti-CA gel may be due to higher hydrolysis rates[24] since the concentration of the metal ion is lower, and changes in pH. Also the water content is higher for the Ti-CA gel compared to the Ti-TEA gel. This is also seen in the residual weights of the gels since for Ti-CA gel it is lower than Ti-TEA gel so we can conclude that the content of TiO_2 in Ti-TEA is higher than Ti-CA gel.

3.4. Crystallographic characterization

After printing and drying, the films were heated in an O_2 atmosphere at 500–650 °C. The transparent and colorless sintered films are shown in Fig. 2. Both powders obtained by sintering the prepared solutions and films were analyzed by XRD to identify the phases present (Fig. 3). We found that all TiO_2 powders and films are crystalline. At 500 °C, pure anatase phase is formed for both powders and films (Fig. 3a and b), while at 650 °C both Ti-TEA and Ti-CA powders showed a mixture of anatase and rutile phase (see Supporting Information (Fig. S2)). The wider peak width for Ti-TEA powder indicates smaller grain size which is in line with the morphology of the films that will be discussed in Section 3.5. When the sintering temperature for the layers was increased up to 650 °C, a small amount of the rutile phase was detected at 2θ ~28° for the Ti-CA layer (Fig. 3c), while in the case of the Ti-TEA layer still pure anatase is found. Interesting to note is that at 600 °C only anatase phase was found for both films (see Supporting Information (Fig. S3)). It can be seen in Fig. 3b and c that the peak intensities are higher for the Ti-TEA film, which is due to the thickness difference between the films. As will be shown later, a thickness of ~650 nm is obtained for Ti-TEA film and ~85 nm for CA film. When comparing the XRD spectra for the Ti-TEA layer heated at 500 °C and 650 °C, it can be seen that in the case of higher temperature sintering, the overlapping peaks at 2θ ~36° and ~55° can be resolved. This might indicate that the grain size increases with the temperature.

3.5. Morphology

SEM analysis was performed on the final TiO_2 layers under low vacuum to study the influence of the precursor formulation and sintering temperature on the morphology of the printed layers (Fig. 4). In the case of the layer from solution Ti-CA, larger and more elongated grains were present in between more

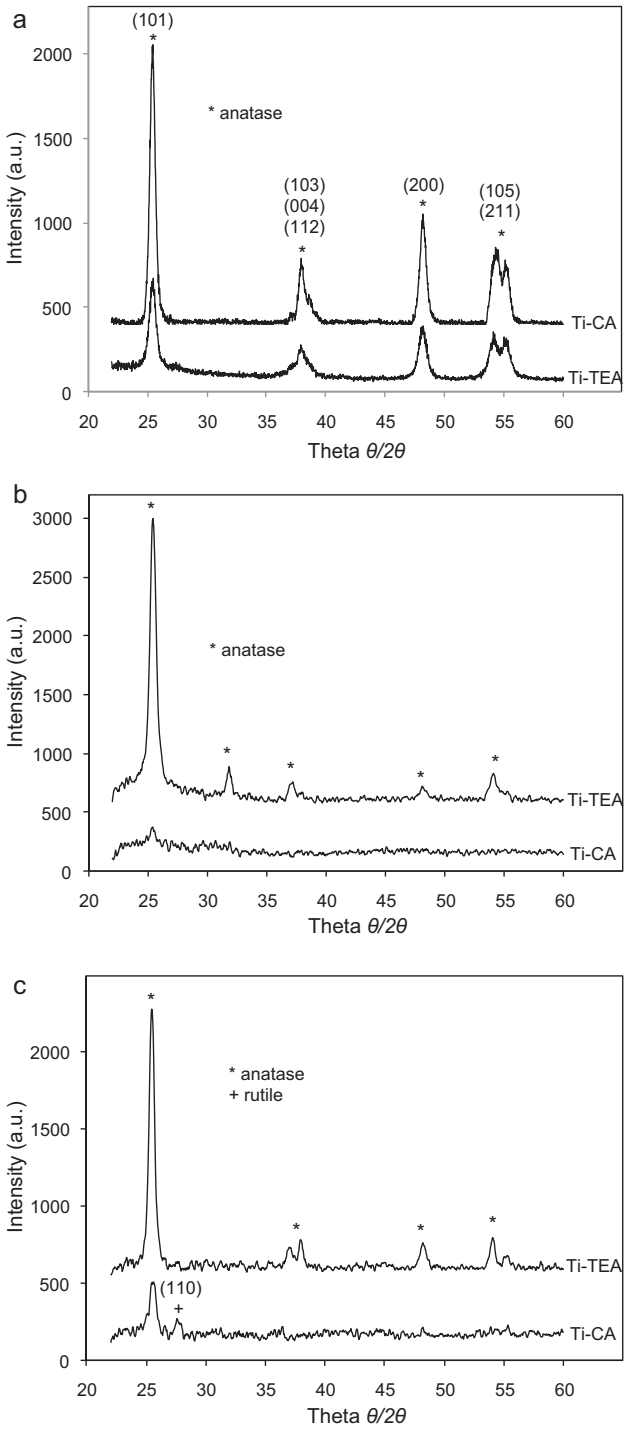

Fig. 3. XRD patterns of the TiO_2 (a) powders, (b) thin films sintered at 500 °C for 1 h and (c) thin films sintered at 650 °C for 1 h, prepared from aqueous solutions Ti-CA and Ti-TEA.

round shaped grains, and their concentration and size seemed to increase further with temperature. The TiO_2 layers obtained from solution Ti-TEA exhibited a smoother and a porous surface. The surface roughness of both films appeared to increase with temperature.

In order to determine the grain size and roughness of the films, non-contact AFM measurements were performed, and the results were analyzed using the WSxM 4.0 software program[25]

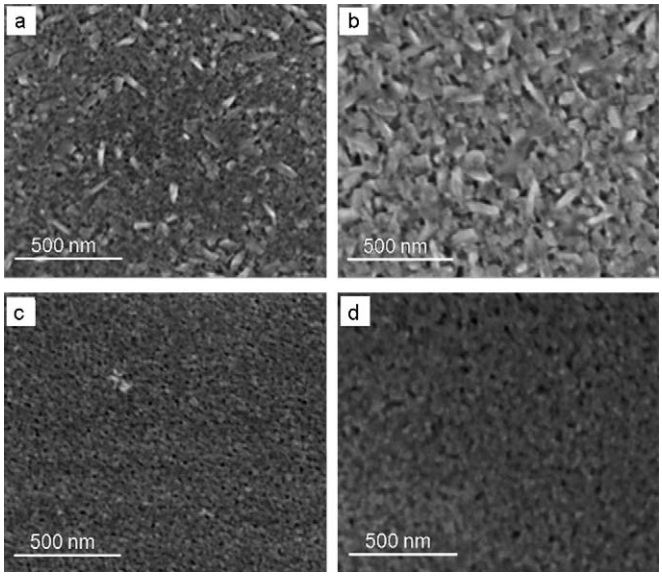

Fig. 4. SEM micrographs of surfaces of different TiO_2 films on glass prepared from solution Ti-CA sintered for 1 h at (a) 500 °C, (b) 600 °C and from solution Ti-TEA sintered for 1 h at (c) 500 °C and (d) 600 °C.

(Fig. 5). For TiO_2 films sintered at 500 °C (Fig. 5a and c), the grain size was estimated at 90–100 nm for Ti-CA and 45–50 nm for Ti-TEA films. The RMS surface roughness measured on an area of 5.0 μm × 5.0 μm, was 6.6 nm for the Ti-CA film and 2.5 nm for the Ti-TEA film. When the sintering temperature was increased to 600 °C, the grain size increased (Fig. 5b and d), and the surface roughness rose to 7.6 nm for the Ti-CA film and 3.9 nm for the Ti-TEA film.

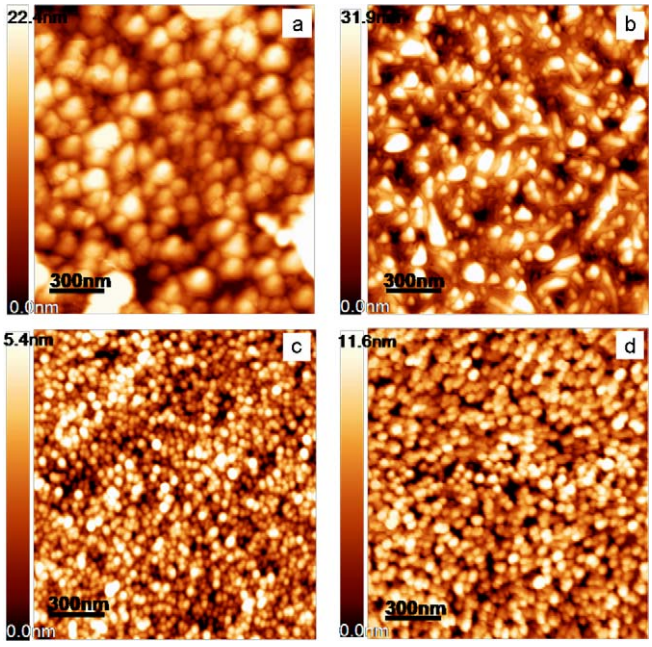

Fig. 5. AFM topography maps of Ti-CA films sintered at (a) 500 °C, (b) 600 °C and Ti-TEA films sintered at (c) 500 °C and (d) 600 °C.

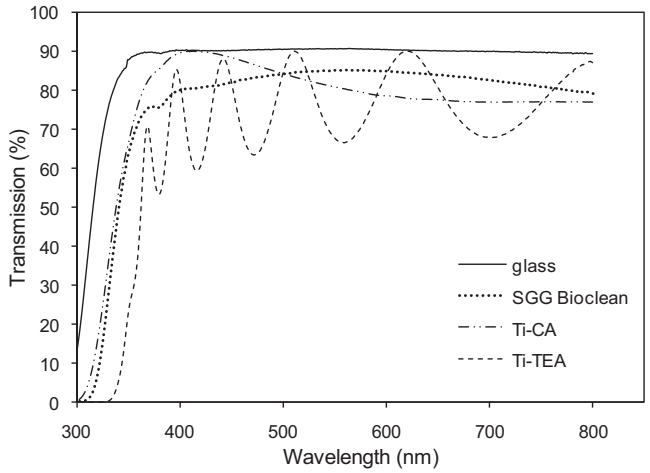

Fig. 6. UV–vis optical transmittance spectra for TiO_2 layers sintered at 500 °C prepared from solution Ti-CA and solution Ti-TEA.

3.6. Transparency and thickness of TiO_2 films

UV–vis spectroscopy was used to examine the transparency of the films (Fig. 6). As a reference, both uncoated microscopy slide glass and commercial self-cleaning window glass from Saint-Gobain (SGG Bioclean[26]) was used. For the Ti-CA film, the transmittance at 500 nm drops from 90% for pure glass to 80% after depositing TiO_2. For SGG Bioclean, the transmittance behaves very similar to Ti-CA film. In the case of the Ti-TEA film, on average, a slightly lower transparency is found. Clear interference fringes were found in the wavelength range 360–800 nm for Ti-TEA film, which are the result of interference between rays reflected from the air-film and film-substrate optical interfaces.[13] From these, we calculated a layer thickness of 546 ± 30 nm based on the formula of Manifacier and Swanepoel.[27,28] In the case of Ti-CA film, the interference fringes are less clear and only two maxima and one minimum can be observed which are not enough to calculate a correct value for the layer thickness.[29–32] Yet, we can estimate a thickness of approximately 100 nm from the spectrum.

From ellipsometry, a layer thickness of ±85 nm for Ti-CA and of ±600 nm for Ti-TEA film, is found, which is in line with the thickness values calculated from the UV–vis spectrum. The thickness of the commercial SGG layer was found to be even thinner for the Ti-CA layer, i.e. about 50 nm. These different results in terms of layer thickness for the two precursor solutions, relate to the different characteristics of the solution such as viscosity, Ti^{4+} concentration, and the used printing parameters (see Table 1). In the case of Ti-TEA, a much larger volume of precursor solution per area can be printed due to reasonable differences in rheology and wetting and spreading behavior.

The refractive index found from ellipsometry is 1.95 for the Ti-CA film and 2.01 for the Ti-TEA film at a wavelength of 632.80 nm. The values lie in the range reported previously for thin, sol–gel derived, TiO_2 films,[20,33,34] but are smaller than the value reported for bulk TiO_2 (~2.54)[29] which can be related to the defects in the layers and a certain degree of porosity.

3.7. Photocatalytic activity

To evaluate the photocatalytic activity of the two TiO_2 films sintered at 500 °C, we compared them with a reference sample film of Degussa P25 made by doctor blade coating[35] and a sample of commercially available SGG Bioclean.[26] The photocatalytic decomposition of methyl orange is studied as a function of time by measuring the change in the absorbance of a solution or the dye in contact with TiO_2 under UV illumination. The selection of methyl orange as specific azo-dye is firstly based on the fact that it is easy to follow its degradation through spectrophotometry. Furthermore, it is also an important effluent of textile industry.[36,37] Finally, methyl orange is preferred over methylene blue because it does not exhibit absorption bands near the irradiation wavelength of the lamps, which excludes the occurrence of side reactions[38–40] where the decomposition of the dye is promoted by exciting the molecules prior to transfer of electrons to the TiO_2 layer. Therefore, it is reasonable to conclude that the photocatalytic process follows a pseudo first-order kinetic mechanism, as described by the following equation[41]:

$$\ln\left(\frac{C}{C_0}\right) = -kt \quad (1)$$

where C is the concentration of methyl orange after photocatalysis time t, C_0 is the initial methyl orange concentration, and k is the kinetic constant of the reaction. The graphical representation of this equation, for uncoated microscopic glass (UNC-G) and three different photocatalytic films and of the same geometrical area is depicted in Fig. 7a. Because of oxygen depletion, the first points are not on the lines. For the uncoated glass the initial increase of the absorbance is due to the evaporation of water since it does not absorb UV, and the temperature in the chamber rises up to 60 °C by UV irradiation. The kinetic constants k of photocatalysis were found to be $k_{CA} = 3.01 \times 10^{-4} \pm 0.02 \times 10^{-4}\,min^{-1}$ for films prepared with citric acid and $k_{TEA} = 4.70 \times 10^{-4} \pm 0.03 \times 10^{-4}\,min^{-1}$ for Ti-TEA films. The opaque, doctor blade titania film was found to exhibit a kinetic constant k_{DB} of $60.45 \times 10^{-4} \pm 0.47 \times 10^{-4}\,min^{-1}$. The performance comparison of Ti-CA and Ti-TEA with the Degussa P25, doctor blade (DB) deposited films clearly indicates the difference between transparent, highly packed thin films comparing to the opaque, lower density doctor blade films. In (heterogeneous) photocatalysis, the "available" photocatalyst surface area is the most important factor to affect the photocatalytic performance. Degussa P25 TiO_2 is an industrially produced powder with aggregates that exceeds the micron size level and thus creates a rough film with extended surface height disparities and high thickness. Subsequently, the photocatalyst surface area that can absorb the dye molecules is large and the photocatalytic efficiency is high.[42] On the other hand, our chemical solution process produces films consisting of nanosized, densely packed grains with a low surface roughness and only a low fraction of the incoming UV-light is absorbed in sol–gel TiO_2 films. Yet, these sol–gel films are transparent and mostly prominent for real-life application, where the TiO_2 film cannot alter the

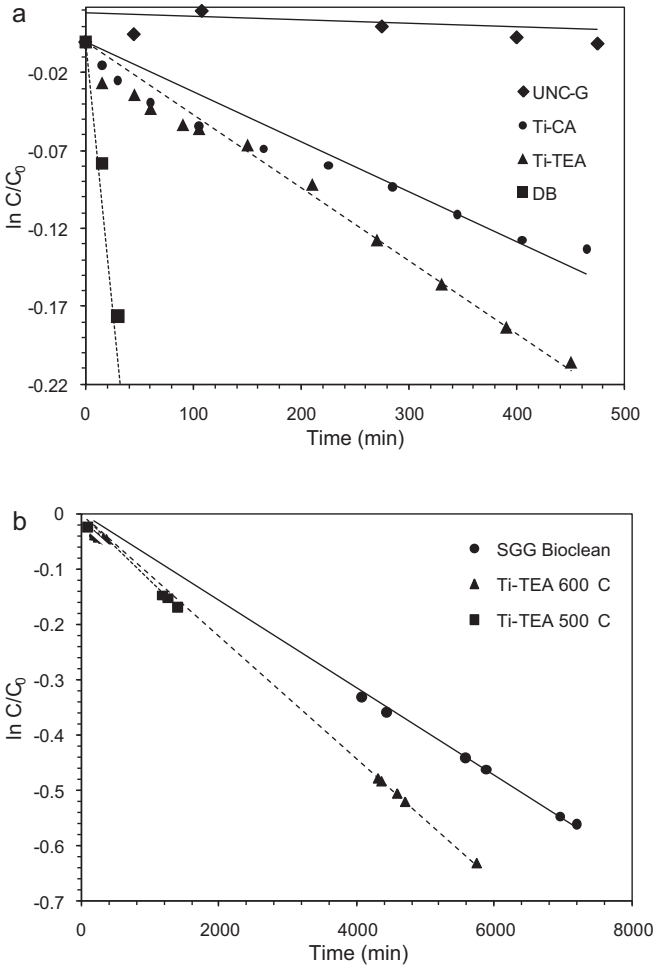

Fig. 7. Kinetics of the photocatalytic degradation of methyl orange: (a) using 0.8 cm^2 uncoated microscopic glass (UNC-G), 0.8 cm^2 TiO_2 films derived from Ti-CA precursor, Ti-TEA precursor, and commercial Degussa P25 titania powder immobilized by applying the doctor blade method (DB); (b) using 2 cm^2 commercial Saint-Gobain titania coated glass, 2 cm^2 TiO_2 films derived from Ti-TEA precursor sintered at 500 °C and 600 °C.

appearance of the substrate to be deposited on. The absorbance of Ti-TEA coated glass is measured under dark conditions without generating UV light, and the result shows that there is no significant decrease of methyl orange for TiO_2 coated glass under dark conditions (see Supporting Information (Fig. S4)).

The difference in photocatalytic efficiency for the Ti-CA and Ti-TEA films is mainly related to the effect of thickness. From the UV–vis transmittance spectra (Fig. 6), it can be clearly seen that at 360 nm, the wavelength used for UV illumination, the transmittance of the TEA layer (41%) is much lower than for the CA layer (77%). From this difference in absorption between the two layers, one expects an increased efficiency for the TEA compared to CA layer. It is generally accepted that increased thickness of titania films supports better photocatalytic efficiency.[43–46] Yet, we also found from SEM and AFM that the Ti-TEA film exhibits a lower roughness and smaller grain size than the Ti-CA films. Smaller grain size (45–50 nm) and a porous surface mean higher active surface and thus better photocatalytic activity. This might suggest that from a morphological

Table 2
Properties of the TiO_2 thin films prepared by ink-jet printing from aqueous precursor solutions.

Solution	Crystallization temp. [°C]	Crystal phase[a]	Refractive index[a]	Thickness [nm][a]	Kinetic constants for photocatalytic activity [min^{-1}]	Film uniformity[a]
Ti-CA	490	A	1.95	±85	$3.01 \times 10^{-4} \pm 0.02 \times 10^{-4}$	Transparent, dense, 90–100 nm grain size, RMS = 6.6 nm
Ti-TEA	500	A	2.01	±600	$4.70 \times 10^{-4} \pm 0.03 \times 10^{-4}$	Transparent, dense, 45–50 nm grain size, RMS = 2.5 nm

[a] For the films sintered at 500 °C, A is anatase.

point of view, Ti-CA films could be more active than Ti-TEA. Therefore, we will also further pursue the preparation of thicker Ti-CA layers.

In Fig. 7b, we show a comparison between the prepared Ti-TEA thin film sintered at 500–600 °C and a commercial SGG Bioclean Saint-Gobain glass which is known as coated by chemical solution derived, transparent, and photocatalytically active layer. Both show a higher activity for the decomposition of methyl orange which might be related to a large difference in thickness between the active layers. Ti-TEA layers are >500 nm thick while typically, the TiO_2 layer obtained by chemical vapour deposition is only 50 nm thick.

In order to sum up the results, the physicochemical properties with the photocatalytic activity of TiO_2 films are summarized in Table 2.

4. Conclusion

Homogeneous, transparent, and thin TiO_2 films have been obtained by a chemical solution deposition method using water as the primary solvent and non-toxic substances such as citric acid and triethanolamine as stabilizing agents. These water based and environmentally friendly TiO_2 solutions can be deposited on glass substrates by ink-jet printing, which is a new technique allowing cheap and fast deposition and avoiding material waste. After sintering the printed layers between 500 °C and 650 °C, transparent TiO_2 layers are obtained. The effect of synthesis conditions, complexing agent, pH and jettability of the solutions, phase formation and surface morphology of the coatings was investigated, and the photocatalytic activity of the TiO_2 layers was compared. Pure anatase phase titania is observed in the coatings when heated up to 600 °C. When TEA is used as complexing agent, the grain size is smaller and the surface roughness is lower than for CA based layer. In the case of Ti-TEA, thicker layers can be produced due to differences in rheology and adaptation of the printing parameters. Surface roughness and porosity increase with sintering temperature. The films clearly exhibit excellent photocatalytic activity when compared with commercially available TiO_2 coated glasses. This work clearly shows that TiO_2 layers prepared by combining aqueous chemical solution deposition route with ink-jet printing can be a suitable alternative to current photocatalytically active self-cleaning glasses coated by TiO_2 using expensive techniques as chemical vapor deposition, thermal methods, and sputtering.

Acknowledgements

This research was carried out under the Interuniversity Attraction Poles Programme IAP/VI-17 (INANOMAT) financed by the Belgian State, Federal Science Policy Office and EFECTS, a project funded by the European Union, FP7-NMP-2007-SMALL-1 grant no. 205854. The authors thank Olivier Janssens (Ghent University) for XRD and SEM analysis. Supporting Information is available online from Wiley InterScience or from the author.

Appendix A. Supplementary data

Supplementary data associated with this article can be found, in the online version, at doi:10.1016/j.jeurceramsoc.2010.12.033.

References

1. Carp O, Huisman CL, Reller A. Photoinduced reactivity of titanium dioxide. *Prog Solid State Chem* 2004;**32**:33–177.
2. Diebold U. The surface science of titanium dioxide. *Surf Sci Rep* 2003;**48**:53–229.
3. Fujishima A, Zhang X. Titanium dioxide photocatalysis: present situation and future approaches. *Comp Rend Chim* 2006;**9**:750–60.
4. Ohya T, Nakayama A, Shibata Y, Ban T, Ohya Y, Takahashi Y. Preparation and characterization of titania thin films from aqueous solutions. *J Sol–Gel Sci Technol* 2003;**26**:799–802.
5. Yoon KH, Noh JS, Kwon CH, Muhammed M. Photocatalytic behaviour of TiO_2 thin films prepared by sol–gel process. *Mater Chem Phys* 2006;**95**:79–83.
6. Truijen I, Van Bael MK, Van den Rul H, D'Haen J, Mullens J. Synthesis of thin dense titania films via an aqueous solution–gel method. *J Sol–Gel Sci Technol* 2007;**41**:43–8.
7. Truijen I, Van Bael MK, Van den Rul H, D'Haen J, Mullens J. Preparation of nanocrystalline titania films with different porosity by water-based chemical solution deposition. *J Sol–Gel Sci Technol* 2007;**43**:291–7.
8. Li C, Zheng Z, Zhang F, Yang S, Wang H, Chen L, et al. TiO_{2-x} films prepared by ion beam assisted deposition. *Nucl Instrum Methods Phys Res B* 2000;**169**:21–5.
9. Saini KK, Sharma SD, Chanderkant, Kar M, Singh D, Sharma CP. Structural and optical properties of TiO_2 thin films derived by sol–gel dip coating process. *J Non-Cryst Solids* 2007;**353**:2469–73.
10. Nagai H, Hasegawa M, Hara H, Mochizuki C, Takano I, Sato M. An important factor for controlling the photoreactivity of titania: O-deficiency of anatase thin films. *J Mater Sci* 2008;**43**:6902–11.

11. Yamamoto S, Sumita T, Sugiharuto, Miyashita A, Naramoto H. Preparation of epitaxial TiO_2 films by pulsed laser deposition technique. *Thin Solid Films* 2001;**401**:88–93.
12. Watanabe A, Tsuchiya T, Imai Y. Selective deposition of anatase and rutile films by KrF laser chemical vapor deposition from titanium isopropoxide. *Thin Solid Films* 2002;**406**:132–7.
13. Addamo M, Augugliaro V, Di Paola A, Garcia-Lopez E, Loddo V, Marci G, Palmisano L. Photocatalytic thin films of TiO_2 formed by sol–gel process using titanium tetraisopropoxide as the precursor. *Thin Solid Films* 2008;**516**:3802–7.
14. Ohya T, Ito M, Yamada K, Ban T, Ohya Y, Takahashi Y. Aqueous titanate sols from Ti-alkoxide-α-hydroxycarboxylic acid system and preparation of titania films from the sols. *J Sol–Gel Sci Technol* 2004;**30**:71–81.
15. Guillard C, Beaugiraud B, Dutriez C, Herrmann J, Jaffrezic H, Jaffrezic-Renault N, Lacroix M. Physicochemical properties and photocatalytic activities of TiO_2-films prepared by sol–gel methods. *Appl Catal B: Environ* 2002;**39**:331–42.
16. Djaoued Y, Taj R, Bruning R, Badilescu S, Ashrit PV, Bader G, Vo-Van T. Study of the phase transition and the thermal nitridation of nanocrystalline sol–gel titania films. *J Non-Cryst Solids* 2002;**297**:55–66.
17. Djaoued Y, Badilescu S, Ashrit PV, Bersani D, Lottici PP, Robichaud J. Study of anatase to rutile phase transition in nanocrystalline titania films. *J Sol–Gel Sci Technol* 2002;**24**:255–64.
18. Legrand-Buscema C, Malibert C, Bach S. Elaboration and characterization of thin films of TiO_2 prepared by sol–gel process. *Thin Solid Films* 2002;**418**:79–84.
19. Kuznetsova IN, Blaskov V, Znaidi L. Study on the influence of heat treatment on the crystallographic phases of nanostructured TiO_2 films. *Mater Sci Eng B* 2007;**137**:31–9.
20. Sheng Y, Liang L, Xu Y, Wu D, Sun Y. Low-temperature deposition of the high-performance anatase-titania optical films via modified sol–gel route. *Opt Mater* 2008;**30**:1310–5.
21. Atkinson A, Doorbar J, Hudd A, Segal DL, White PJ. Continuous ink-jet printing using sol–gel "ceramic" inks. *J Sol–Gel Sci Technol* 1997;**8**:1093–7.
22. Yoshimura M, Gallage R. Direct patterning of nanostructured ceramics from solution – differences from conventional printing and lithographic methods. *J Solid State Electrochem* 2008;**12**:775–82.
23. Hardy A, Van Werde K, Vanhoyland G, Van Bael MK, Mullens J, Van Poucke LC. Study of the decomposition of an aqueous metal-chelate gel precursor for $(Bi,La)_4Ti_3O_{12}$ by means of TGA-FTIR, TGA-MS and HT-DRIFT. *Thermochim Acta* 2003;**397**:143–53.
24. Van de Velde N, Arin M, Lommens P, Poelman D, Van Driessche I. Characterization of the aqueous peroxomethod for the synthesis of transparent TiO_2 thin films. *Thin Solid Films* 2010 [Ref. number: TSF-D-10-00355].
25. Horcas R, Fernandez JM, Gomez-Rodriguez J, Colchero J, Gomez-Herrero J, Baro AM. WSXM: a software for scanning probe microscopy and a tool for nanotechnology. *Rev Sci Instrum* 2007;**78**:8.
26. SGG Bioclean - self cleaning glass, Saint-Gobain Glass UK Ltd, Eggborough East Riding Yorkshire DN14 OFD, www.selfcleaningglass.com.
27. Manifacier JC, Gasiot J, Fillard JP. A simple method for the determination of the optical constants n, k and the thickness of a weakly absorbing thin film. *J Phys E: Sci Instrum* 1976;**9**:1002–4.
28. Swanepoel R. Determination of the thickness and optical constants of amorphous silicon. *J Phys E: Sci Instrum* 1983;**16**:1214–22.
29. Tigau N, Cuipina V, Prodan G. The effect of substrate temperature on the optical properties of polycrystalline Sb_2O_3 thin films. *J Cryst Growth* 2005;**277**:529–35.
30. Poelman D, Smet PF. Methods for determination of the optical constants of thin films from single transmission measurements: a critical review. *J Phys D: Appl Phys* 2003;**36**:1850–7.
31. Gordijn A, Loffler J, Arnoldbik WM, Tichelaar FD, Rath JK, Schropp REI. Thickness determination of thin (∼20 nm) microcrystalline silicon layers. *Solar Energy Mater Solar Cells* 2005;**87**:445–55.
32. Takeuchi M, Yamashita H, Matsuoka M, Anpo M, Hirao T, Itoh N, Iwamoto N. Photocatalytic decomposition of NO on titanium oxide thin film photocatalysis prepared by an ionized cluster beam technique. *Catal Lett* 2000;**66**:185–7.
33. Wang Z, Halmersson U, Kall PO. Optical properties of anatase TiO_2 thin films prepared by aqueous sol–gel process at low temperature. *Thin Solid Films* 2002;**405**:50–4.
34. Nishide T, Sato M, Hara H. Crystal structure and optical property of TiO_2 gels and films prepared from Ti-EDTA complexes as titania precursors. *J Mater Sci* 2000;**35**:465–9.
35. Arabatzis IM, Antonaraki S, Stergiopoulos T, Hiskia A, Papaconstantinou E, Bernard MC, Falaras P. Preparation, characterization and photocatalytic activity of nanocrystalline thin film TiO_2 catalysts towards 3,5-dichlorophenol degradation. *J Photochem Photobiol A: Chem* 2002;**149**:237–45.
36. Zollinger H. *Color chemistry*. 3rd ed. New York: VCH Publishers; 1987.
37. Chung KT, Cerniglia CE. Mutagenicity of azo dyes–structure–activity–relationships. *Mutat Res* 1992;**277**:201–20.
38. Kiriakidou F, Kondarides DI, Verykios XE. The effect of operational parameters and TiO_2-doping on the photocatalytic degradation of azo-dyes. *Catal Today* 1999;**54**:119–30.
39. Zhang F, Zhao J, Shen T, Hidaka H, Pelizzetti E, Serpone N. TiO_2-assisted photodegradation of dye pollutants – II. Adsorption and degradation kinetics of eosin in TiO_2 dispersions under visible light irradiation. *Appl Catal B: Environ* 1998;**15**:147–56.
40. Chen F, Xie Y, Zhao J, Lu G. Photocatalytic degradation of dyes on a magnetically separated photocatalyst under visible and UV irradiation. *Chemosphere* 2001;**44**:1159–68.
41. Alekabi H, Serpone N. Kinetic-studies in heterogeneous photocatalysis. 1. Photocatalytic degradation of chlorinated phenols in aerated aqueous-solutions over TiO_2 supported on a glass matrix. *J Phys Chem* 1988;**92**:5726–31.
42. Mills A, Lepre A, Elliott N, Bhopal S, Parkin IP, O'Neill SA. Characterisation of the photocatalyst Pilkington Activ^{TM}: a reference film photocatalyst? *J Photochem Photobiol A: Chem* 2003;**160**:213–24.
43. Tada H, Tanaka M. Dependence of TiO_2 photocatalytic activity upon its film thickness. *Langmuir* 1997;**13**:360–4.
44. Yu J, Zhao X, Zhao Q. Effect of film thickness on the grain size and photocatalytic activity of the sol–gel derived nanometer TiO_2 thin films. *J Mater Sci Lett* 2000;**19**:1015–7.
45. Legrini O, Oliveros E, Braun AM. Photochemical processes for water-treatment. *Chem Rev* 1993;**93**:671–98.
46. Gratzel M. Sol–gel processed TiO_2 films for photovoltaic applications. *J Sol–Gel Sci Technol* 2001;**22**:7–13.